Mechanical and physical properties of hybrid Cu-graphite Composite prepared via powder metallurgy technique

En. Fouad R. Mohialdeen
Kirkuk Cement Plant
Email: Fouad.Ramadhan1978@yahoo.com

Abstract

Copper -graphite composites are widely used in a great number of engineering applications such as brushes, switches, sliding bearings, self-lubricating bearings, etc. due to their good thermal and electrical conductivity and excellent tribological properties as compared with other structural materials. There are ongoing attempts in manufacturing copper composites with better properties to enhance their efficiency and increase their effective life.

Present research aims to prepare hybrid 95 wt.% copper –5 wt.% graphite composites reinforced with yttria and tin particles by powder metallurgy technique and to study their effects on mechanical and physical properties of the prepared composites.

Powder mixture was mixed by ball mill mixer at 100 r.p.m for 120 min with (5/1) balls to powder ratio. The powder mixture was cold pressed at 700 MPa for 30 sec, followed by sintering at 900 ˚C for one hour. In the first stage, Yttria(Y_2O_3) was added with (2, 4, 6, 8, 10)wt% to pure copper(Cu) and to (95%Cu-5%Gr) matrices. Typical composite of this stage was ((95%Cu-5%Gr)-4%Y2O3.

In the second stage, tin (Sn) was added with (2, 4, 6, 8, 10)wt% to pure copper and((95%Cu-5%Gr)-4%Y2O3 matrices. Typical composite of this stage was ((95%Cu-5%Gr)-4%Y2O3)-6%Sn. The results showed that hardness and true porosity of the composites increases with increasing yttria content. On the other hand both thermal and electrical conductivity of the composites decreases with increasing yttria content. It was also found that (95 wt.% Cu- 5 wt.% Gr) – Y_2O_3 composites have always lower wear rate than plain Cu-Y_2O_3 composites.

Keywords: Hybrid Copper-Graphite Composites, powder metallurgy

Mechanical and physical properties of hybrid Cu-graphite Composite prepared via powder metallurgy technique

الخواص الميكانيكية والفيزياوية لمتراكب هجين ذات اساس من النحاس- الكرافيت المحضرة بطريقة ميتالورجيا المساحيق

الخلاصة

تستخدم متراكبات النحاس- الكرافيت على نطاق واسع في عدد كبير من التطبيقات الهندسية مثل الفرش الكهربائية، والمفاتيح، ومحامل الانزلاقية ، ومحامل التزييت الذاتي وغيرها بسبب امتلاكها الموصلية الحرارية والكهربائية الجيدة والخواص الترايبولوجي الممتازة بالمقارنة مع المواد التركيبية الأخرى. هناك محاولات مستمرة في تصنيع مركبات النحاس ذات خواص أفضل لتحسين كفاءتها وزيادة عمرها بشكل مؤثر. هدف البحث الجاري ان نصنع متراكبات هجينية ذات الارضية من النحاس (95%) والكرافيت (5%) بتقنية ميتالورجيا المساحيق ودراسة تاثيرالمضافات على الخواص الميكانيكية والفيزياوية لمتراكبات المصنعة تم خلط المساحيق بواسطة خلاط (طاحونةكروية) لمدة 120 دقيقة وبسرعة 100 دورة\دقيقة ونسبة الكرات الى المساحيق (1\5).تم كبس خليط المساحيق تحت ضغط 700 ميكاباسكال لمدة 30 ثانية واتبعت بالتلبيد في 900 درجة مئوية لمدة ساعة واحدة. . اضيفت اليتريابنسب وزنية (2, 4, 6, 8, 10) الى ارضية النحاس النقي والى (95%Cu-5%Gr). المتراكب المثالي في هذه المرحلة هو ((95%Cu-5%Gr-4%Y2O3)). في المرحلة الثانية, اضيفت القصدير بنسب وزنية (2, 4, 6, 8, 10)الى ارضية النحاس النقي والى ارضية(95%Cu-5%Gr-4%Y2O3)). المتراكب المثالي في هذه المرحلةهو ((95%Cu-5%)-4%Y_2O_3)-6%Sn .

اظهرت النتائج ان الصلادة والمسامية الحقيقية تزداد مع زيادة محتوى اليتريا. من جهة اخرى كل من توصيلية الحرارية والكهربائية تقل مع زيادة محتوى اليتريا. وكذلك وجدت معدل البلى للمتراكبات Y_2O_3 – (Gr %wt. 5 -Cu %wt. 95) دائما اقل من معدل البلى للمتراكبات $Cu-Y_2O_3$.

1. Introduction

In the last few years, several attempts have been done to reinforce copper in order to improve its mechanical properties. Copper is one of the most promising metal because of its high electrical and thermal conductivity, superior corrosion and oxidation resistance. However due to its relatively high ductility, low yield strength, weak creep resistance and low hardness, it is necessary when increasing its mechanical properties be careful not to greatly affect its electrical properties [1]. Structural materials composed of matrix material and reinforcement material are called composite materials which combine the properties of two or more components [2, 3]. Using single reinforcement in copper matrix may sometimes lead to the deterioration of its physical and mechanical properties. To overcome these losses in copper properties, hybrid composites are prepared from two or more different types of reinforcements with copper matrix. Oxides of metals like aluminium, cerium, yttrium and zirconium are often used for this purpose as fine and uniformly distributed dispersoid particles in soft and ductile copper matrix. Such composites find applications as electrical contacts, resistance-welding tips, lead

wires, continuous casting moulds, etc. [4]. The most common routes for particle-reinforced Cu matrix composites include casting and powder metallurgy methods. Powder metallurgy (PM) is preferred to casting because of low agglomeration, low segregation and good wettability [5, 6]. PM processing

includes mixing, pressing and sintering [7]. Graphite plays a significant role in advanced energy materials with excellent tribological properties [8]. Copper–graphite composites, produced by powder metallurgy processes are now widely used in tribological engineering parts, such as bearings, and electrical contact parts, notably carbon brushes for engines and generators[9]. [10] found that mixing variables and powder characteristics such as particle shape and particle size distribution have great effects on sintered density and microstructural homogeneity of Cu-(Sn,Pb) composites. [11] studied the effect of processing parameters and amount of additives on the mechanical properties and wear resistance of copper-based composite. They found that increasing the graphite content up to 5 wt% increase the wear resistance of the Cu-(Sn, Pb) composites. [12] achieved near full densification in copper – graphite composite through pressing at 700 MPa for 30 sec, followed by sintering at 900 ˚C for 1 hr. [13] studied the effect of process parameters on the hardness and microstructure of copper – graphite composites prepared by powder metallurgy route. He found that the optimum compacting pressure, sintering temperature and sintering time for conventional sintering were 700 MPa, 900 ˚C and 1 hr. respectively. [14] studied the tribological properties of Cu matrix composites reinforced with Fe, Gr, Sn, ZrO_2 and SiO_2) prepared by PM that is used in dry friction clutch. They found that improper material formulations caused inferior properties particularly with high sintering temperatures. High Sn contents caused swelling of the sintered materials as well as tribological properties (coefficient of friction and wear resistance). It was found that the investigated materials were insensitive to sintering temperatures in the range (800-900) ˚C but they were strongly influenced by chemical compositions.

2. Experimental Procedure

2.1 Used Materials

Electrolytic copper powder (≤ 63 μm in size with 99.7% purity), graphite powder (≤ 53 μm in size with 99.9 % purity), yttria powder ((10-5) μm in Size with 99.95 % purity) and tin powder (≤ 53μm in size with 99.95 % purity) were selected as metal matrix, soft reinforcement, hard reinforcement and modifier respectively.

2.2 Composite Preparation

Graphite powder was preheated up to 200 ˚C for two hours to get rid of moisture and other volatile substances. Hybrid 95% copper–5% graphite composite is fabricated by powder metallurgy technique and prepared through two stages as illustrated in figures 1 and 2 which represent the flow charts of the experimental procedure in stage 1 and 2 respectively.
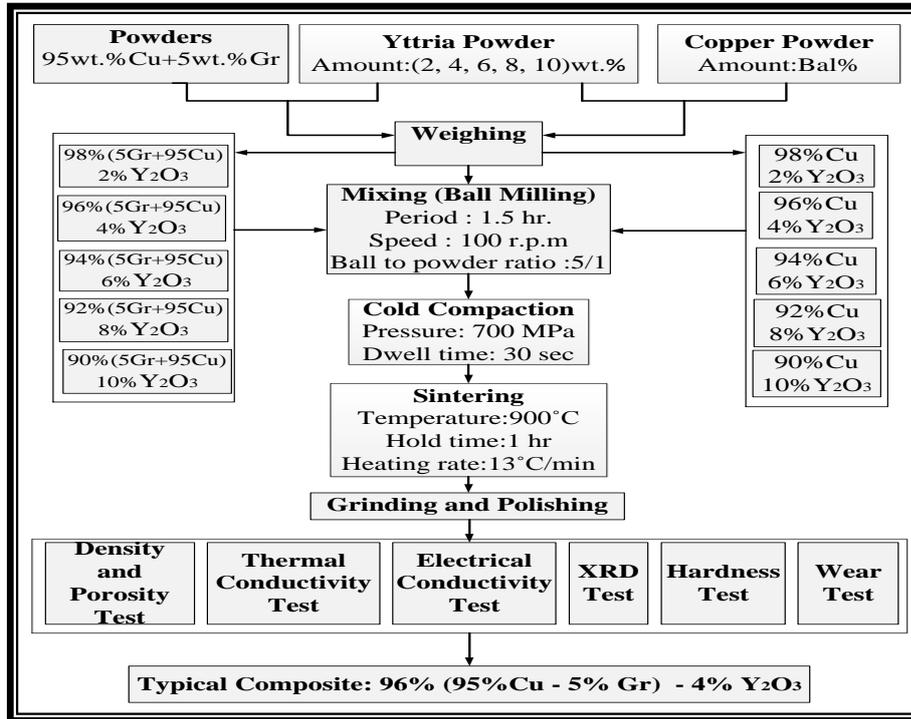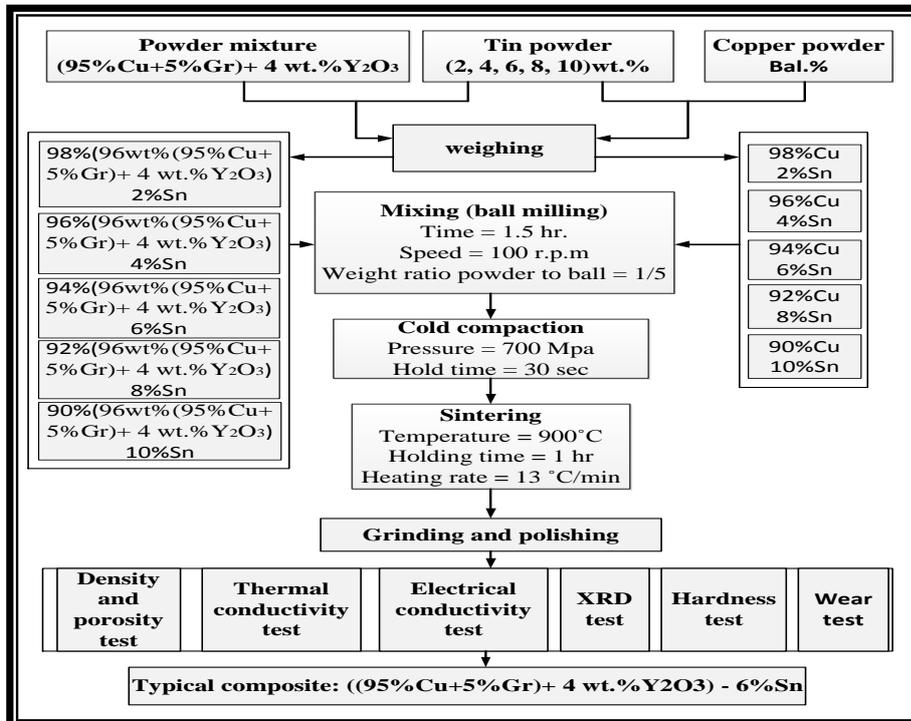
Fig. 1: Flow chart for the experimental procedure of stage-1

Fig. 2: Flow chart for the experimental procedure of stage-2

The powders were mixed by mixing machine (ball milling) as shown in figure (3) for 1.5 hrs at 100 rpm. 8 mm diameter balls were used with 5/1 balls to powder ratio.

The powder mixtures were cold pressed by uniaxial pressing at 700 MPa for 30 sec inside a cylindrical hardened steel die using compaction machine (type: U test, turkey) with capacity 250 KN to produce green compacts with 10 mm in diameter and 7±1 mm in height. The inner surface of the die was lined with thin layer of graphite to avoid the adhesion between die and punch as well as to provide lubrication during ejection of the compact.

Green compacts were sintered at 900 ˚C for 1 hr. with heating rate 13 ˚C/min, followed by cooling inside an electric muffle furnace. To prevent oxidation, the samples were placed in a ceramic container with multilayer graphite powder and gray cast iron chips and are sealed with castable (Alumina + silica) layer and castable magnesium oxide layer as shown in figure (4).This configuration was proved to be effective in oxidation prevention [15]. K-type thermocable was used to measure and control sintering temperature inside the container.
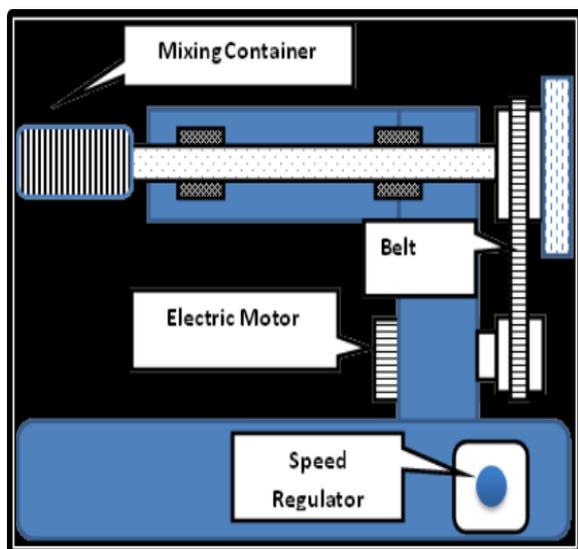

Fig. 3: A sketch for mixing machine
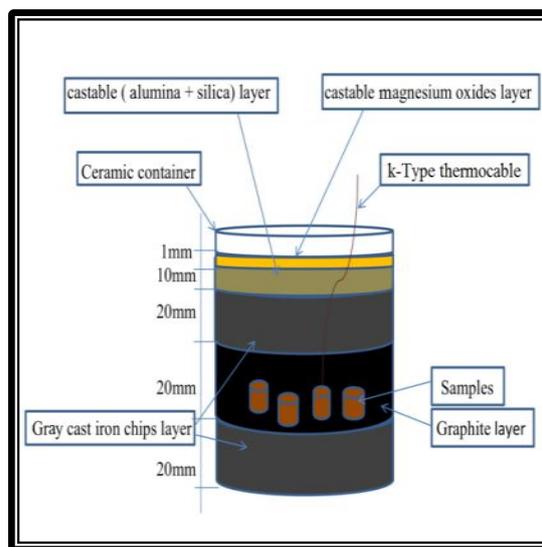
Fig. 4: sintering container

2.3 Performance testing

2.3.1 Hardness Test

The hardness of the sintered compacts was measured using Brinell hardness tester (type: Innovatest, Netherland) at a load of 30 kg and a dwell time of 20 sec using indentation ball of 1 mm diameter. Each hardness value represents an average of ten readings.

2.3.2 Wear Test

Wear test was performed using a pin on disc-tribometer (P.A. Hilton Ltd Company, UK). Sintered compacts represent the pins while hardened steel disc of 218 HB was used as counter disc. Before loading the specimens on the test device, the surface of the hardened steel disc was thoroughly cleaned with acetone. Wear tests were carried out under dry sliding condition and a normal load of 40N. The rotating speed of the steel disc was 350 rpm for 30 min. All experiments were carried out in ambient temperature and relative humidity of 36%. Each specimen was weighed before and after every wear test in an electronic balance with 0.1 mg precision to obtain the weight loss. The wear rate was calculated according to the following formula [16]

$$\text{Wear rate} = \frac{\Delta W}{S} \ (\text{g/cm}) \qquad\qquad ……. \ 1$$

$$\Delta W = W_1 - W_2$$

$$S = 2\pi rnt$$

W_1 = weight of specimen before the test (g)

W_2= weight of specimen after the test (g)

S = sliding distance

r = sliding radius (cm) (from center of the disc to center of the specimen)

n = sliding speed (r.p.m)

t = sliding period (min)

2.3.3 Determination of Relative Density and True Porosity

Sintered or true density of the specimens was determined by Archimedes' principle according to [17]. The procedures were carried out as follows:

1- The test specimens were dried at 150 °C for 1 hr then cooled slowly to room temperature inside the oven. The dry weight of the cooled specimens (W_d) were measured.

2- The suspended weight (W_i) was determined by suspending and sinking the specimen inside flask containing distilled water.

3- The specimens were immersed in boiled distilled water for 5 hrs. then followed by soaking in distilled water for an additional 24 hrs. at room temperature. Subsequently, specimens were weighed

after removing all excess surface water by a moistened, lint-free linen or cotton cloth to obtain weight (W_s).

Relative density and porosity were determined by the following relationships [18, 19, 20]:

$$\text{T.D} = \sum_{i=1}^{n}(\rho_i . x_i) \qquad \dots\dots \quad 2$$

T.D = Theoretical density (g/cm^3)

ρ_i = Density of element in the composite (g/cm^3)

x_i = Percentage of element in the composite

$$\text{B.D.} = \frac{W_d}{W_s - W_i} \times \rho_w \qquad \dots\dots \quad 3$$

B.D. = Bulk density (g/cm^3)

W_d = Dry weight (g)

W_i = Suspended weight (g)

W_S = Saturated weight (g)

ρ_w = Water density = 1 g/cm^3

$$\text{R.D} = \frac{\text{B.D}}{\text{T.D}} \times 100\% \qquad \dots\dots \quad 4$$

R.D = Relative density

$$\text{T.P.} = \frac{\text{T.D.} - \text{B.D.}}{\text{T.D.}} \times 100\% \qquad \dots\dots \quad 5$$

T.P. = True porosity

2.3.4 Thermal and Electrical conductivity Test

Thermal conductivity was determined by using thermal conductivity measurement system (TechQuipment Ltd, UK).The sample was put in the device between two brass blocks; the first block was heated while the second block was cooled by current water. Electric power was applied to supply the required heat energy to heat the sample while a set of thermocouples were used to measure the temperature gradient along the two brass blocks and the supported sample between them. Heating was continued until a steady state condition between the two samples ends (ΔT) was satisfied. Fourier law was applied to calculate the thermal conductivity [20].

$$-\text{K} = \frac{Q}{A \times \frac{\Delta T}{\Delta X}} \qquad \dots\dots \quad 6$$

Where

Q = amount of heat (W) =10 Watt

K = thermal conductivity (W/ (m.k))

ΔT = temperature difference between the two ends of the specimen (m)

Δx = distance between the two thermocouples that measures two points on the sample (m)

A = cross section area of the specimen (m^2)

7

Electrical conductivity of samples was calculated from the thermal conductivity by using Wiedmann-Franz Equation as follows [21, 22].

$$\frac{\lambda}{\sigma T} = L = 2.443 \times 10^{-8} \left(\frac{w.\Omega}{k^2} \right) \qquad \qquad \dots\dots \qquad 7$$

λ = thermal conductivity (W/(K.m))

σ = electric conductivity ($\Omega^{-1}.m^{-1}$)

T = absolute temperature (K)

L = lourinse number = $2.443 \times 10^{-8} \left(\frac{w.\Omega}{k^2} \right)$

2.3.5 XRD Test

X-ray diffraction device (type: SHIMADZU, made in Japan) utilizing copper target was used to observe the formed phases which was identified by comparing the obtained inter-atomic distance values with a standard tables according to ASTM by using analytic program match! 3.

3. Results and Discussion

3.1 Effect of Reinforcement Materials on Relative Density and True Porosity

Figure (5) exhibits the relationship between relative density and reinforcement material (yttria and tin). It can be observed that increasing Y_2O_3 content in Cu-Y_2O_3 composite decreases relative density, where it is reduced from 94% to 86% with 0 and 10 wt.% Y_2O_3 respectively. This is due to the increased porosity content with increasing Y_2O_3 as shown in figure (6). The porosity increase is attributed to the lack of wettability between ceramic materials and copper[23], agglomeration of yttria particles, and to the particles size of both Cu and Y_2O_3 which is near to each other, which prevent Y_2O_3 to act as filler in copper matrix.

On adding Y_2O_3 to (95 % Cu – 5 % Gr) matrix, relative density increases to reach (86 %) with 4 wt.% Y_2O_3. This desirable effect is attributed to the high initial porosity of (95 % Cu- 5 % Gr) composite, which reaches 18% since Y_2O_3 acted as filler in that composite. This effect is enhanced by graphite particles, which help small Y_2O_3 particles to slip toward pore sites. Increasing Y_2O_3 beyond 4 wt.% reduces relative density through the decrease of filling action of Y_2O_3, agglomeration tendency of Y_2O_3 particles and the accompanied increase in porosity, and finally to the insulation effect of both graphite and yttria which reduces consolidation and densification of copper matrix. From the above results, it is found that 4 wt.% Y_2O_3 is the most suitable addition to (95 %Cu- 5 %Gr) from relative density view point.

In figure (5), it is also observed that increasing tin content in both Cu-Sn composites and ((95%Cu-5%Gr)-4%Y_2O_3)-Sn composites increase relative density while true porosity decreases on increasing tin content as shown in figure (6). On sintering at 900 ˚C, tin melts and liquid sintering

mechanism will be activated. Activation of liquid sintering mechanism enhances filling process of porosity, consolidation and densification of composites. Referring to figures (5) and (6) it is observed that Cu-Sn composites have higher density and lower porosity than Cu-Gr-Y_2O_3-Sn composites due to the inherent porosity that accompanies graphite and yttria presence in these composites. However, on increasing tin content the density of both plain Sn-Cu and hybrid Cu- composites becomes near to each other. The same is true for true porosity. This behavior is attributed to the increased activity of tin in porosity filling and densification action with increasing its content.

3.2 Effect of Reinforcement Materials on Thermal and Electrical Conductivity

Figures (7) and (8) show that increasing Y_2O_3 content reduces both thermal and electrical conductivity of Cu-Y_2O_3 composites, where thermal conductivity reduces from (272.837)W/(m.K) to (126.5023) W/(m.K) and electrical conductivity reduces from (38.1164) $(\mu\Omega.m)^{-1}$ to (17.6728) $(\mu\Omega. m)^{-1}$ by increasing yttria content from 0 wt.% to 10 wt.% respectively. This behavior can be attributed to the continuous increase in porosity with increasing yttria content and to the lower thermal and electrical conductivity of yttria are (13 W/(K.m) and 0.04 $(\mu\Omega.m)^{-1}$ respectively). Similar behavior was previously obtained for Cu–Y_2O_3 microcomposites [24].

On the other hand, addition of Y_2O_3 to (95%Cu-5%Gr)composite results in an increase in thermal and electrical conductivity up to 4% Y_2O_3 where these conductivities were increased from (159.1549)W/(m.K) to (179.1504) W/(m.K) and from (22.2345) $\mu\Omega^{-1}.m^{-1}$ to (25.111) $\mu\Omega^{-1}.m^{-1}$ respectively by increasing yttria content from 0 wt.% to 4wt.% respectively. Any addition of yttria after 4wt.% results in continuous reduction in both thermal and electrical conductivities. This behavior represents a direct reflection of true porosity behavior of these composites as shown in figure (6).

Figures (7) and (8) reveal that Cu-Y_2O_3 composites have always higher thermal and electrical conductivity than (95 % Cu -5 % Gr)-Y_2O_3 composites. This is due to the higher porosity level for (95%Cu-5%Gr)-Y_2O_3 composites which acts as insulation sites.

Figure (7) and (8) also reveal the effect of tin content on thermal and electrical conductivity of Cu- Sn and hybrid Cu- Gr-Y_2O_3- Sn composites. It is observed that Sn reduces both thermal and electrical conductivity of Cu- Sn composites where thermal conductivity reduces from (272.8370) W/(m.k) to (165.8701) W/(m.k) and electrical conductivity from 38.1164 $(\mu\Omega.m^{-1})$ to 23.1727 $(\mu\Omega.m)^{-1}$ at 0wt.% and (10)wt% tin respectively. This is due to the lower thermal and electrical conductivity of tin itself and to the Cu_6Sn_5 intermetallic compound that is formed on sintering as is shown in XRD patterns that will be discussed later. Thermal and electrical conductivity of Sn and Cu_6Sn_5 are (227 W/(K.m), 21.7 $(\mu\Omega. m)^{-1}$) [20]and (39 W/(K.m)[25], (5.7) $(\mu\Omega.m)^{-1}$) [27, 28] respectively. While thermal and electrical conductivity of copper are (397 W/(K.m)) and (60 $(\mu\Omega.m)^{-1}$) respectively [20].

On adding tin to hybrid composites, thermal and electrical conductivity firstly increases till 4 wt.%Sn; where thermal and electrical conductivity increase from 169.1504 W/(K.m) to 185.2463 W/(K.m) and from 23.6309 $(\mu\Omega.m)^{-1}$ to 25.8796 $(\mu\Omega.m)^{-1}$ at 0 wt.% and 4 wt.% respectively. This

increase is attributed to reduction in porosity by filling action of tin. After this percentage both thermal and electrical conductivity reduce to (120.230) W/(m.k) and (16.797) $\mu\Omega^{-1}.m^{-1}$ respectively at 10%Sn due to reduction in area fraction of copper matrix.

Figure (7) and (8) also show that both thermal and electrical conductivity of hybrid Cu-Gr-Y_2O_3-Sn composites is always lower than Cu-Sn composites. This is due to the presence of low thermal and electrical conductivity constituents i.e. graphite, and yttria besides tin where their presence is on the account of the reduction in copper matrix with its higher thermal and electrical conductivity.

3.3 Effect of Reinforcement Materials on Hardness

Figure (9) shows the effect of Y_2O_3 addition on Brinell hardness of Cu- Y_2O_3 and (95 wt.% Cu- 5 wt.% Gr) – Y_2O_3 composites. This figure illustrates that increasing yttria content increases the hardness of both composites where Brinell hardness increases from (62.3)HB to (76.2)HB and from (56.4)HB to (67.5)HB by increasing Y_2O_3 content from 0 to 10 wt.% of Cu- Y_2O_3 and (95 wt.% Cu- 5 wt.% Gr) – Y_2O_3 composites respectively. Y_2O_3 increases composite hardness firstly by the hard nature of it particles and their action in hindering the dislocation motion and secondly by their effect as grain growth inhibitor. Furthermore, the great difference in thermal expansion between yttria reinforcement and copper matrix promotes dislocations to be produced and their density to be increased at the interface between reinforcement and matrix. This increase in dislocation density contributes in increasing the composite hardness [29, 30]. It can also be observed from figure (9) that Cu-Y_2O_3 composites are always harder than (95 wt.% Cu- 5 wt.% Gr) – Y_2O_3 composites. This behavior is attributed to the higher porosity level in (95 wt.% Cu- 5 wt.% Gr) – Y_2O_3 composites as shown in figure (6) and to the contribution of graphite particles in reducing composite hardness.

Figure (9) also shows the relationship between tin and the hardness of both copper-tin composites and hybrid copper-graphite-yttria composites. The hardness of both types of composites increases with increasing tin content up to 6wt.% while any further addition of tin beyond 6 wt.% reduces Brinell hardness of both composites. For Cu- Sn composites hardness was found to be (62.3, 64.88, and 58.33) HB at (0, 6 and 10) wt.% Sn respectively. While for Cu- Gr- Y_2O_3-Sn composites, it was found to be (58.3, 69.15, and 61.37) HB at (0, 6, 10) wt.%Sn respectively. Tin addition increases Brinell hardness through reducing porosity, enhanced consolidation and densification by liquid sintering mechanism and partly through the formation of the hard intermetallic compound Cu_6Sn_5 [31]

besides solid solution hardening. However on increasing tin content above 6 wt.% composites hardness decreases due to the soft nature of tin and to the excess formation of Cu_6Sn_5 which precipitates at Cu-Sn interface leading to weak bond between copper matrix and tin reinforcement particles.

3.4 Effect of Reinforcement Materials on Wear Rate

Figure (10) reveals that increasing yttria content in $Cu-Y_2O_3$ composites reduces the wear rate till 6 wt.% where the wear rate reduces from (1.7×10^{-7}) g/cm to (1.2×10^{-7}) g/cm at 0 and (6) wt.% Y_2O_3 respectively. Any further increase in yttria addition beyond 6 wt.% increases the composite wear rate. Reduction in wear rate with increasing yttria content up to 6 wt.% is due to the corresponding increase in composite hardness with increasing Y_2O_3 content as shown in figure (9). However increasing Y_2O_3 content beyond 6 wt.% leads to the formation of yttria agglomerates which weaken the bond between yttria and the matrix as well as increasing of the porosity. These agglomerates have harmful effects on the bonding between reinforcement and matrix besides their harmful effects on the nature of the interface where microporosity prefers to form at these sites [24, 32]. Addition of yttria to (95wt%Cu-5wt%Gr) composite reduces wear rate till (4)%Y_2O_3 where wear rate reaches (0.56×10^{-7}) g/cm. Increasing yttria content over (4)wt% increases wear rate continuously to reach (1×10^{-7})g/cm at (10) wt%.

Figure (10) also reveals that (95% Cu- 5% Gr) – Y_2O_3 composites have always lower wear rate than plain $Cu-Y_2O_3$ composites. This is due to the combined effect of both graphite which contributes in reducing wear rate through its lubrication effect and yttria particles through their high hardness. (95 % Cu- 5 % Gr) – Y_2O_3 composites is found to give the lowest wear rate among all other composites with some reduction in thermal and electrical conductivity, so it is selected as basic composition for the addition of tin as an additional constituent.

In figure (10), it is observed that wear rate of both copper-tin composite and hybrid copper composites reduces with increasing tin contents till 6 wt% tin. Where it decreases from (1.7×10^{-7}) g/cm to (0.7×10^{-7}) g/cm and from (0.57×10^{-7}) g/cm to (0.18×10^{-7}) g/cm for both composites respectively. This is attributed to the same factors that increase Brinell hardness of these composites. Increasing tin content above 6wt.% increases wear rate remarkably for both types of composites. This is attributed mainly to precipitation the brittle Cu_6Sn_5 intermetallic compound at Cu- Sn interfaces, which weakens them leading to dislocation or fragmentation of these particles from rubbed surface easily under the effect of friction forces and increases wear rate of these composites.

Throughout the present study, it is found that hybrid copper composite with 5 wt% Gr- 4 wt% Y_2O_3-6 wt% Sn is considered to be the best among all other composites where it shows the lowest wear rate and good thermal and electrical conductivity.

11

3.5 X-Ray Diffraction (XRD) Test

Figure (11) shows the XRD pattern of pure copper compact. All the prominent peaks (high intensity) belong to metallic copper. No any sign of oxidation.

Figure (12) shows the XRD pattern of Cu-5wt.%Gr composite. It is observed that the strong peaks belongs to metallic copper and relatively weak peak (low intensity) belongs to graphite. Not any reaction between copper matrix and graphite reinforcement was taking place on sintering.

Figures (13) and (14) show XRD patterns of Cu-6wt.%Y_2O_3 and Cu-10wt.%Y_2O_3 composites respectively. It is observed that the presence of the intermetallic $Cu_2Y_2O_5$ compound due to occurrence of partial reaction between yttria and copper. Peaks of copper are also the prominent peaks in these composites. Absence of copper oxide peaks confirms that no oxidation takes place during sintering.

Figures (15) and (16) show XRD for (95%Cu-5%Gr)-4%Y_2O_3 and (95%Cu-5% Gr)-10%Y_2O_3 composites respectively. Clear major peaks of Cu, Gr, Y_2O_3 and $Cu_2Y_2O_5$ are observed in these composites. Increasing yttria content increases intensity of yttria and $Cu_2Y_2O_5$ peaks.

Figures (17), (18) and (19) represent the XRD patterns of Cu-4%Sn, Cu-6%Sn and Cu-10%Sn composites respectively. Strong peaks of Cu_6Sn_5 was observed in all composites. Peak intensity increases with increasing Sn content. No sign of metallic Sn was observed. This is due to the complete reaction between copper and tin on sintering.

Figure (10) shows the XRD pattern of the hybrid (95wt%-5wt%)-10wt%Y_2O_3-6wt%Sn composite. Major peaks were found to belong to metallic Cu, Gr, Y_2O_3, Sn, $Cu_2Y_2O_5$ and Cu_6Sn_5. Moreover, peak intensity of Cu was found in this composite is lower than these present in other composites due to the presence of high amounts of other constituents and the reaction between some of these constituents and copper.

12
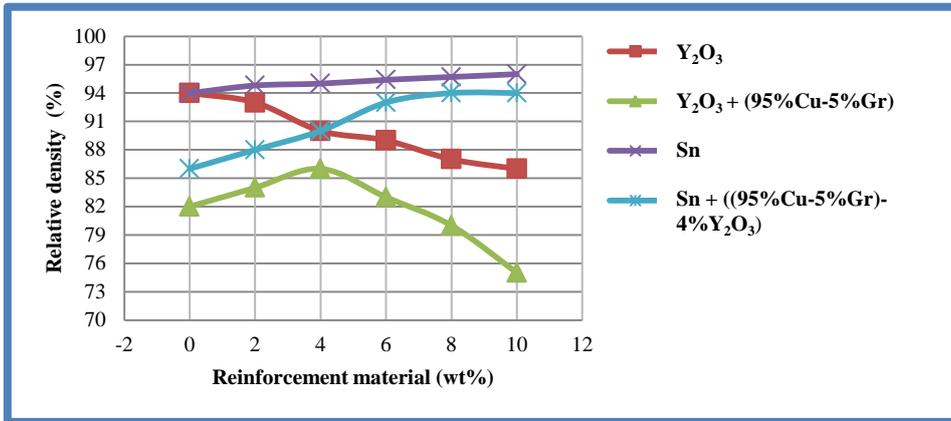
Fig. 5: Relationship between relative density and reinforcement materials
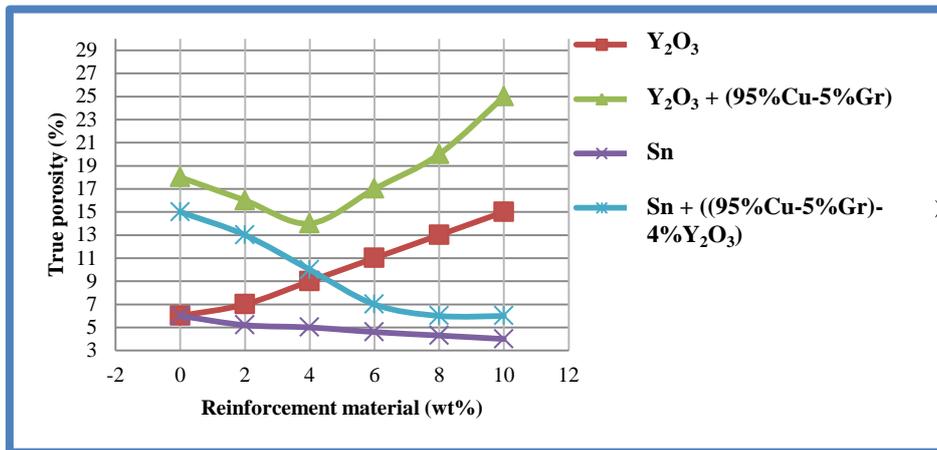

**Fig. 6: Relationship between true porosity and reinforcement materials**
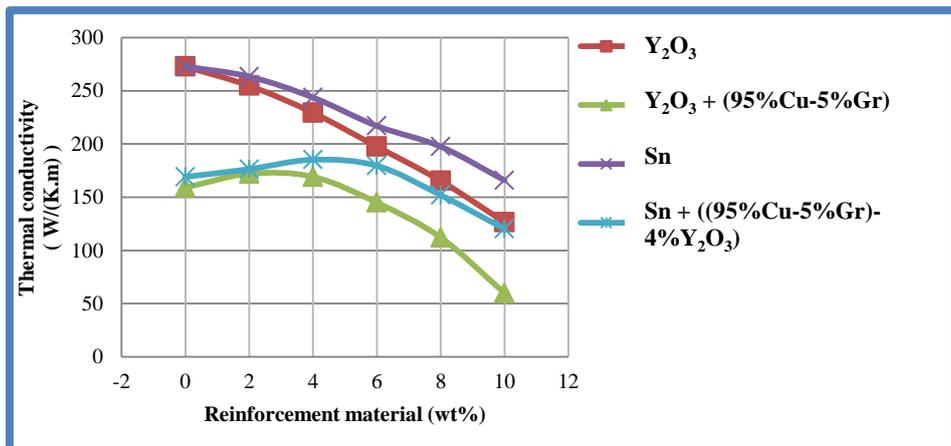
Fig. 7: Relationship between thermal conductivity and reinforcement materials
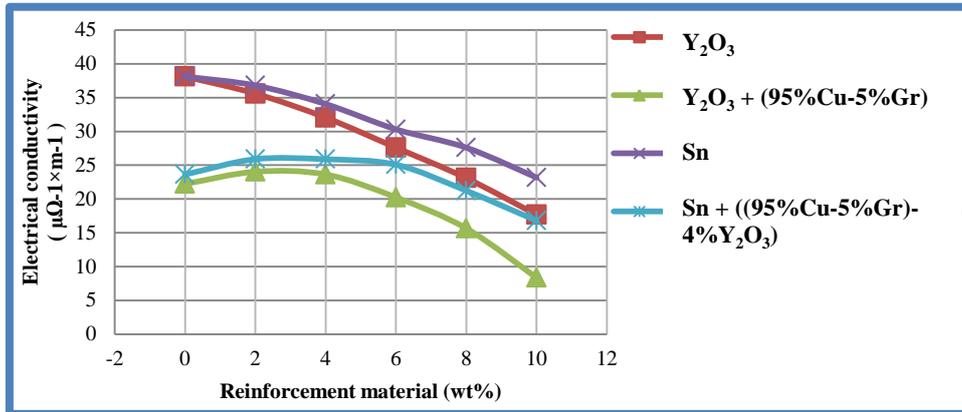
Fig. 8: Relationship between electrical conductivity and reinforcement materials
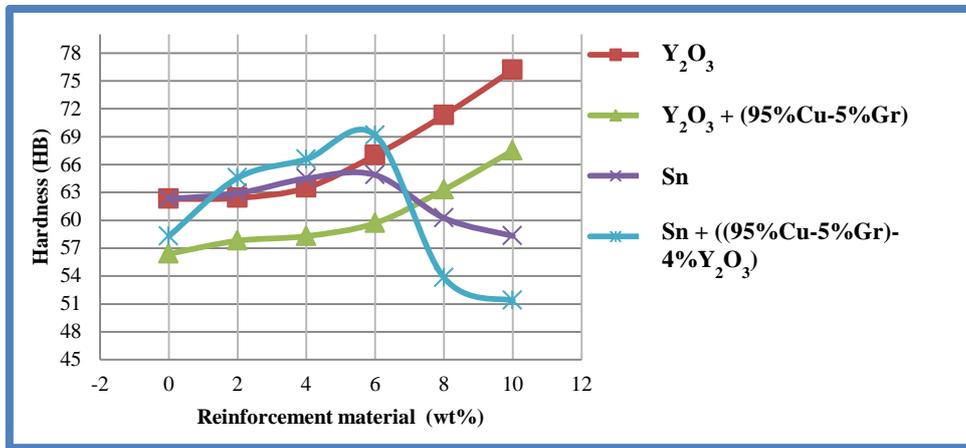
**Fig. 9: Relationship between the hardness and reinforcement materials**
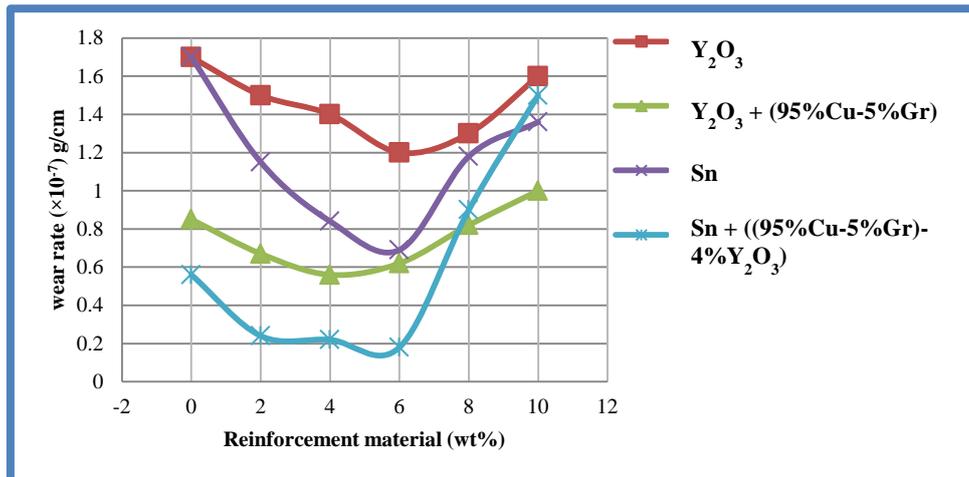
Fig. 10: Relationship between the wear rate and reinforcement materials
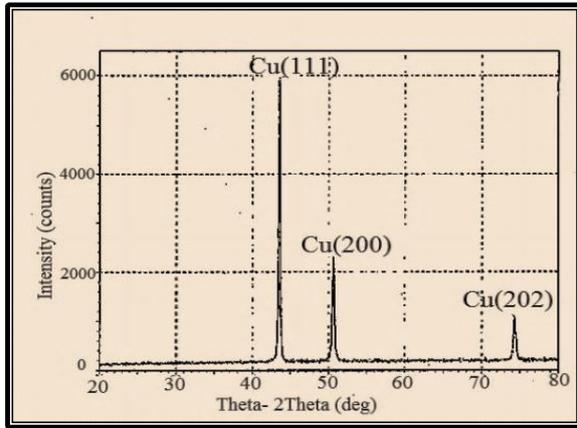
Fig. 11: XRD of pure copper compacts
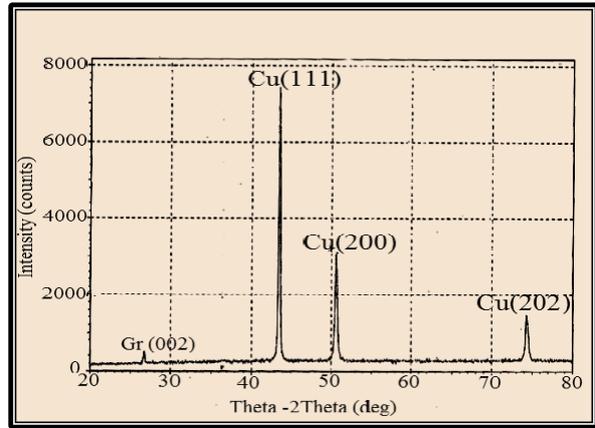
Fig. 12: XRD of Cu-5%Gr composite
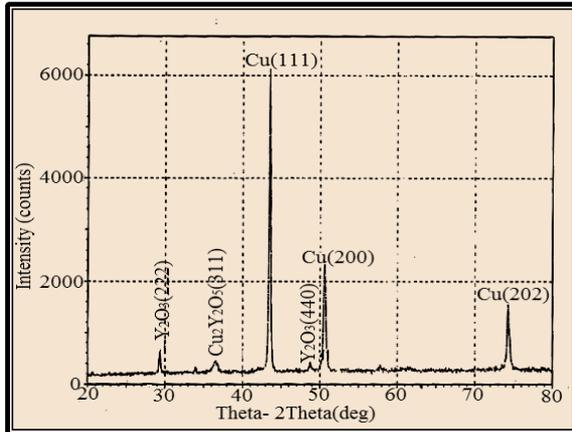
Fig. 13: XRD of Cu-6%Y$_2$O$_3$ composite
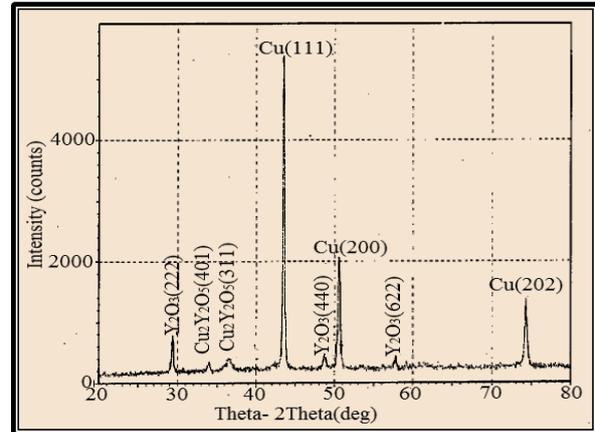
Fig. 14: XRD of Cu-10%Y$_2$O$_3$ composite
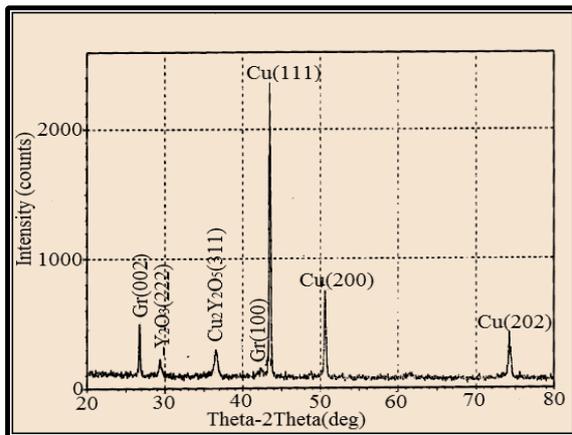
Fig. 15: XRD of Cu-5%Gr-4%Y$_2$O$_3$ composite
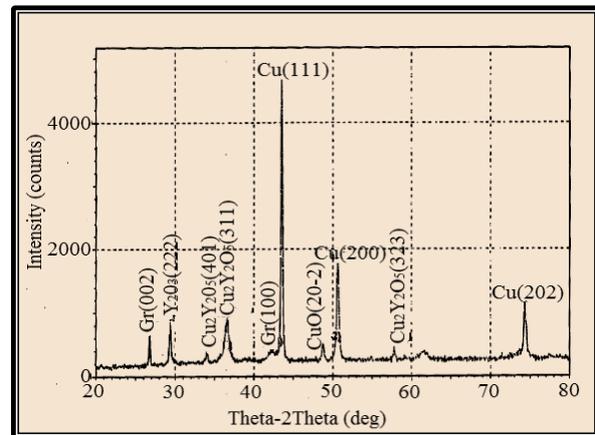
**Fig. 16: XRD of Cu-5%Gr-10%Y$_2$O$_3$ composite**
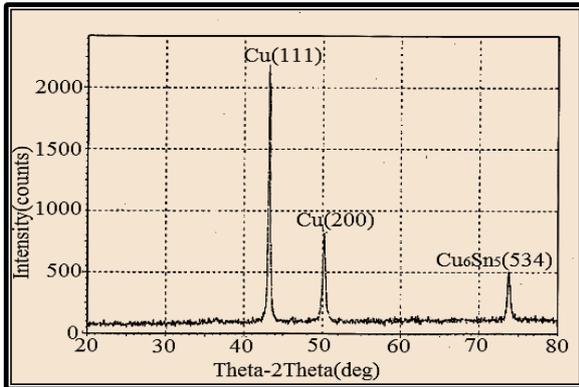
Fig. 17: XRD of Cu-4%Sn
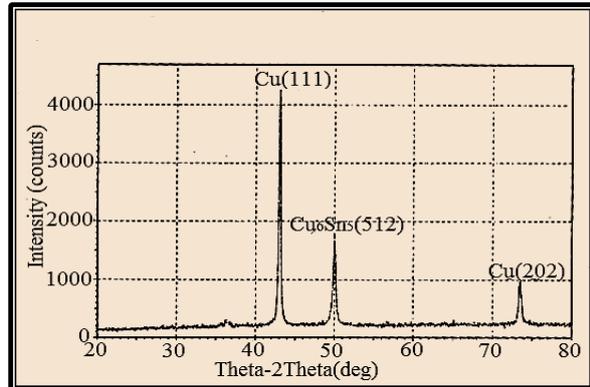

Fig. 18: XRD of Cu-6%Sn
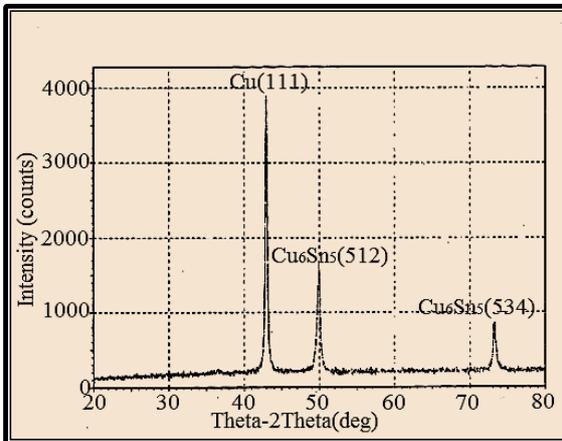

Fig. 19: XRD of Cu-10%Sn
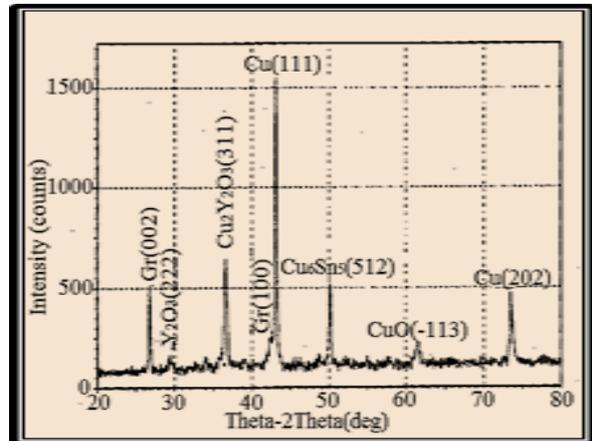
Fig. 20: XRD of ((95%Cu-5%Gr)-10%Y$_2$O$_3$)-6%Sn

Conclusions

1. Hybrid Copper-graphite composites have been successfully prepared by powder metallurgy technique.

2. (95 wt.% Cu- 5 wt.% Gr) – Y$_2$O$_3$ composites have always lower wear rate than plain Cu-Y$_2$O$_3$ composites.

3. Hardness and true porosity of the composites increases with increasing yttria content.

4. Thermal and electrical conductivity of the composites decreases with increasing yttria content.

5. Thermal and electrical conductivity of Cu-Gr-Y$_2$O$_3$-Sn composites is always lower than those of Cu-Sn composites.

6. Addition of tin to both pure copper and (95%Cu-5%Gr)-4%Y$_2$O$_3$ composites reduces true porosity.

7.

8. Increasing tin content up to 6 wt.% increases the composite hardness despite the the matrix composition.

9. Thermal and electrical conductivity of Cu-Sn composites reduce with increasing of tin content.

10. Thermal and electrical conductivity of hybrid $((95\%Cu\text{-}5\%Gr)\text{-}4\%Y_2O_3\text{-}Sn$ composite increases with increasing tin content till 4%Sn.

11. The best composite which found in this work is $((95\% \text{ Cu-}5\% \text{ Gr})\text{-}4\% \text{ Y}_2O_3)\text{-}6\% \text{ Sn}$ which has true porosity (7%), relative density (93%), hardness (69.15 HB), wear rate (0.18×10^{-7} g/cm), thermal conductivity (179.507 W/k.m) and electrical conductivity (25.0778 $\mu\Omega^{-1}.m^{-1}$).

References

1- A.Molina, A. Torres-Islas, S. Serna, M. Acosta-Flores R.A. Rodriguez-Diaz1 and J. Colin **"Corrosion, Electrical and Mechanical Performance of Copper Matrix Composites Produced by Mechanical Alloying and Consolidation"** International Journal of Electrochemical Science (2015) **Vol. 10, PP. 1728 - 1741.**

2- Daniel B. Miracle, L. Steven **"Composites"** Volume 21, ASM Handbook, the ASM International Handbook Committee (2001).

3- Izabela Firkowska, André Boden, Benji Boerner, Stephanie Reich **"The Origin of High Thermal Conductivity and Ultralow Thermal Expansion in Copper–Graphite Composites"** Nano Letters., Department of Physics, Freie Universität Berlin, Germany, **VOL. 15 , PP. 4745–475, (2015).**

4- Joshi, P. B., Rehani, Bharati, Naik, Palak, Patel, Swati, Khanna, P. K. **"Studies on Copper-Yttria Nanocomposites: High-Energy Ball Milling Versus Chemical Reduction Method"** Journal of Nanoscience and Nanotechnology, **Volume 12, Number 3, PP. 2591-2597, (2012).**

5- B. D. Long, R. Othman, Hussain Zuhailawati and M. Umemoto **"Comparison of Two Powder Processing Techniques on the Properties of Cu-NbC Composites"** Journal of Advances in Materials Science and Engineering **VOLUME 2014, 6 PAGES (2014).**

6- Mohammadmehdi Shabania, Mohammad Hossein Paydara, Reza Zamirib, Maryam Goodarzic, Mohammad Mohsen Moshksara **"Microstructural and Sliding Wear Behavior of SiC-Particle Reinforced Copper Matrix Composites Fabricated by Sintering and Sinter-Forging Processes"** Journal of Materials Research and Technology **Volume 5, PP. 5–12 (2016).**

7- N. Leemaa, P. Radhab, S.C. Vettivelc, H. Khanna Nehemiah **"Characterization, Pore Size Measurement and Wear Model of a Sintered Cu–W Nano Composite Using Radial Basis Functional Neural Network"** Journal of Materials and Design, **VOL. 68, PP. 195–206 (2015).**

8- Fadhil A.Chyad, Ibrahim R.Agoal, Mahdi M.Mutter **"Effect of Addition SiC Particles on the Hardness and Dry Sliding Wear of the Copper-Graphite Composite"** The Iraqi Journal For Mechanical And Material Engineering, **Vol.12, No.2, (2012).**

9- Amrishraj.D, Senthilvelan.T **"Modelling and Optimization of Sliding Wear Behaviour of Copper-Graphite Composites"** Proceedings of Second International Conference on Advances in Industrial Engineering Applications, Anna University, Chennai (2014).

10- Dongdong Gu, Yifu Shen **"Effects of Dispersion Technique and Component Ratio on Densification and Microstructure of Multi-Component Cu-Based Metal Powder in Direct Laser Sintering"** Journal of Materials Processing Technology **VOL. 182, PP. 564–573, (2007).**

11- Montasser Dewidar, G.T. Abdel-Jaberb, Mahmoud Bakrey, and Hussien Badry **"Effect of Processing Parameters and Amount of Additives on the Mechanical Properties and Wear Resistance of Copper-Based Composite"** International Journal of Mechanical & Mechatronics Engineering **Vol:10 No. 03, (2010).**

12- Yongping Jin, Ming Hu **"Densification of Graphite/Copper Compound Powders"** PP. 1131-1135, 978-1-4244-9439-2/11© IEEE , (2011)

13- Chandana Priyadarshini Samal **"Microstructure and Mechanical Property Study of Cu-graphite Metal Matrix Composite Prepared by Powder Metallurgy Route"** master degree, Department of Metallurgical and Materials Engineering National Institute of Technology Rourkela Rourkela-769 008, Orissa, India, (2012).

14- Jirapat Prapai, Monnapas Morakotjinda, Thanyaporn Yotkaew, Bhanu Vetayanukul, Ruangdaj Tongsri, Panaya Kamsuwan, Masahiko Yoshino **"Tribological Properties of PM Cu- Based Dry Friction Clutch"** Journal of Materials science and technology, Trans Tech Publication, Switzerland **VOL. 545, PP. 163-170 (2013).**

15- Farouk M.Mahdi, Raed N.Razooqi, Saif S. Irhayyim **"Effect of Graphite Content and Milling Time on Physical Properties of Copper - Graphite Composites Prepared by Powder Metallurgy Route"** Australian Journal of Basic and Applied Sciences, **PP. 245-255, 7(12) Oct 2013.**

16- Nikhilesh Chawla , Krishan K. Chawla **"Metal Matrix Composites"** Library of Congress Cataloging in Publication Data, Springer Science Business Media, University of Alabama at Birmingham (2006).

17- ASTM C373 – 88 **"Standard Test Method for Water Absorption, Bulk Density, Apparent Porosity, and Apparent Specific Gravity of Fired White Ware Products",** Reapproved (2006).

18- Goutam Dutta , Dipankar Bose **"Effect of Sintering Temperature on Density, Porosity and Hardness of a Powder Metallurgy Component"** International Journal of Emerging Technology and Advanced Engineering , ISSN **2250-2459, Vol. 2 , No. 8 ,PP. 121-123 August (2012).**

19- Shobhit Jain, R.S Rana, Prabhash Jain **"Study of Microstructure and Mechanical Properties of AL-Cu Metal Matrix Reinforced with B_4C Particles Composite"** International Research Journal of Engineering and Technology, **Volume: 03, PP.499-504, (2016).**

20- William D. Callister, Jr. **"Fundamentals of Materials Science and Engineering"** Fifth Edition, (2001).

21- Zeinb Abdel Hamid , Sayed F. Moustafa , Fatma A. Morsy , Nevien Abdel Atty Khalifa , Fatma Abdel Mouez "**Fabrication and Characterization Copper / Diamond Composites for Heat Sink Application Using Powder Metallurgy**" Natural Science , **, Vol. 3 , PP. 936-947. (2011).**

22- Jaroslav Kováčik , Štefan EmmerAffiliated , Jozef Bielek **"Cross-Property Connections for Copper–Graphite Composites"** Slovak University of Technology, **Volume 227, PP. 105-112 (2016).**

23- S. Barzilai, M. AizenshteinN. Froumin, N. Frage **"Y2O3/(Cu–Me) Systems (Me=Al, Ti): Interface Reactions and Wetting"** Journal of Materials Science, August 2006, **Vol. 41, Issue 16, PP. 5108-5112, (2006).**

24- J.P.Stobrawa, Z.M. Rdzawski, W.J. Głuchowski **"Microstructure and Properties of Nanocrystalline Copper - Yttria Microcomposites"** Journal of Achievements in Material and Manufacturing Engineering, **VOL. 24, ISSUE 2, PP. 83-86 (2007).**

25- Syugo Miyake, Yasuko Nagano, Aya Miyake, Hiroyuki Takamatsu, Takashi Kita **"Spatially Resolved Thermal Conductivity of Intermetallic Compounds Measured by Micro-Thermo-reflectance Method"** Journal of Japan Institutes of Metals, **Vol. 74, No. 11, PP. 740-745, (2010).**

26- Vincent, C., J.F. Silvain, J.M. Heintz, N. Chandra, **"Effect of Porosity on the Thermal Conductivity of Copper Processed by Powder Metallurgy"** Journal of Physics and Chemistry of Solids, Vol. 7: PP. 499-504, (2012).

27- Jiři Podzemsky, Vaclav Papez, Jan Urbanek, Karel Dusek **"Influence of Intermetallic Compounds on RF Resistance of Joints Soldered with Lead Free Alloys"** Dept. of Electrotechnology, Czech Technical University, Technique 2, 166 27 Prague, Czech Republic, **VOL. 21, NO. 2, PP. 573-579 JUNE 2012.**

28- John Jones **"Tin Whiskers and Copper/Tin Intermetallics"** Alter Technology Group 1000 Lakeside, North Harbour, Portsmouth Hampshire, UK, *john.jones@altetechnology.com* (2006).

29- Hamed Simchia, A. Simchia **"Tensile and Fatigue Fracture of Nanometric Alumina Reinforced Copper with Bimodal Grain Size Distribution"** Journal of Materials Science and Engineering A **VOL. 507, PP. 200–206 (2009).**

30- Riccardo Casati and Maurizio Vedani **"Metal Matrix Composites Reinforced by Nano-Particles—A Review"** journal of metals, **VOL. 4, PP. 65-83 (2014).**

31- J. R. J. Fields, S. R. Low, G. K. Lucey, Jr. **"Physical and Mechanical Properties of Intermetallic Compounds Commonly Found in Solder Joints"** Published in Metal Science of Joining, Proceedings of TMS Symposium, Cincinnati, Volume 358, Issues 1–2, PP. 134–141 (1991).

32- Reddy G. Chandrakanth, K. Rajkumar, Sivanandam Aravindan **"Fabrication of Copper–TiC–Graphite Hybrid Metal Matrix Composites Through Microwave Processing"** journal of advanced manufacturing technology, **VOL. 48, PP. 645–653, (2010).**